Military Technical College
Kobry El-Kobbah,
Cairo, Egypt.

13th International Conference on Applied Mechanics and Mechanical Engineering.

TRIBO BEHAVIOUR OF POLYMER NANOCOMPOSITES (MODELLING AND EXPERIMENTS)

GNANAMOORTHY R. and SRINATH S.

ABSTRACT

Addition of nanosize reinforcements to polymer matrix is a recent approach to improve the matrix strength and modulus and widen the application of polymers and their composites for many structural applications. Polymer nanocomposites are new specialty plastic compounds, which have reinforcement having at least one dimension in the nanometre scale (10^{-9} m) in a polymer matrix. Many researchers have reported the significant increase in the strength and modulus due to the addition of nanoparticles. The tribo behaviour of an engineering material is another aspect that needs to be understood clearly and decides the performance of many engineering components such as gears, bearings etc. This paper describes the tribo behaviour of polyamide base nanocomposites. The analytical model developed to predict the coefficient of friction is also described.

Department of Mechanical Engineering, Indian Institute of Technology Madras, Chennai 600 036, India. Email: gmoorthy@iitm.ac.in

INTRODUCTION

Wear causes surface damage, results in loss in performance, material loss, energy dissipation, and increased vibration. Although the friction and wear of thermoplastic polymers have some fundamental similarities with metals, there are also significant differences in the wear mechanisms involved and the level of friction and wear. Some unique advantages of polymers as tribo materials compared to metals are low friction coefficient, self-lubrication, good chemical resistance, easy fabrication, able to accommodate shock loading and misalignment. Hence, polymers are slowly replacing metals in the machine elements where friction and wear links to the application. The suitability of polymers in tribological applications largely depends on the mechanical strength, modulus and wear resistance. Most commonly used thermoplastics for structural and tribological applications are polyamides (PA), polycarbonates (PC), polyacetal (POM), polyetheretherketone (PEEK), and polyether sulphone (PES). Most polymers have poor mechanical properties when compared to metals. In order to improve the mechanical properties, polymers are reinforced with fibres. Reinforcing polymer with glass, aramid and carbon fibres improves dimensional stability, strength, and modulus, wear resistance, thermal resistance, creep resistance and fatigue endurance. The reinforcement efficiency depends on the interaction between the fibre/filler and the matrix, rigidity and the aspect ratio of the filler. The size of reinforcement in short fibre reinforced composites is in micrometer range, which is large compared with the size of polymer molecule, which is in nanometre range. The significant difference in size between the two components results in loss in the reinforcement efficiency.

Polymer nanocomposites thus emerged as new specialty plastic compounds, which has reinforcement phase having at least one dimension in the nanometre scale (10^{-9}m) in a polymer matrix. When nano sized filler is incorporated in polymer matrix, the reinforcing efficiency greatly increases due to high interaction of polymer molecules with the filler and improves the mechanical properties. Polymer nanocomposites exhibit a drastic improvement in the modulus, strength, flammability and barrier property than the pristine polymer. The improvements in the properties are achieved at low filler content, which means that there is no appreciable change in the density of the composite (LeBaron, *et al*., 1999; Jordan *et al*., 2005).

Dry sliding wear occurs when surfaces slide in air without any lubricant. Most polymers have a low coefficient of friction and self-lubricating capacity, and are used in applications where dry sliding occurs and in situations where external lubrication cannot be provided. A few literatures are available on the dry sliding of nanocomposites with the nano sizes particles such as silicon carbide (SiC), silicon nitride (Si_3N_4) etc. Wang *et al*. (1996) reported the friction and wear properties of nanometre Si_3N_4 filled polyetheretherketone (PEEK). The nanometre Si_3N_4 filled composite considerably reduced the friction coefficient and wear compared to pure PEEK. Formation of tenacious transfer film on the ring surface influenced the tribo behaviour. The wear mechanisms of various kinds of silicon carbide (SiC) filled PEEK composites are investigated by Xue *et al*. (1997). All the fillers reduced the coefficient of friction and wear but the wear mechanisms involved were different. Among the fillers studied, nano sized SiC filler was effective in improving the tribological properties of PEEK composites due to the formation of smooth transfer layer on the counterface. Schwartz and Bahadur (2000) studied the tribological properties of polyphenylene sulphide (PPS) filled with alumina nanoparticles. As the percentage of filler increased above an

optimum value, the composite material experienced more wear than the unfilled counterpart. Unlike the previous work in PEEK, the coefficient of friction increased monotonically with increasing filler concentrations. The friction behaviour of ZnO/PTFE composite was found similar to that of pure PTFE [Li *et al*. (2002)]. Filling of nano sized ZnO affects the microstructure of PTFE and prevents the destruction of the PTFE banded structure.

This paper describes the friction and wear characteristics of the polyamide base nanocomposites. The analytical model developed to predict the coefficient of friction is also described.

MATERIALS DEVELOPMENT AND TRIBO TEST DETAILS

The materials under consideration are polyamide base containing different quantities of nanosized organoclay. The organoclay used was montmorillonite clay modified with 2 methyl, 2 hydrogenated tallow quaternary ammonium chloride having a individual platelet size of the clay ranging from about 0.5 x 0.5 x 0.001 microns to about 0.8 x 0.8 x 0.001 microns in size while the clay bundles is of the order of about 75 microns. The nanocomposite granules were prepared by melt mixing using a twin-screw extruder. The granules were preheated at 333 K for 4 h to remove the moisture before injection moulding to tribo test samples at an injection pressure of 125 MPa. Many components made of polymeric materials operate under dry sliding conditions. Dry sliding friction and wear tests were conducted using the pin-on-disk tribometer at different normal loads varying from 30 to 60 N. The sliding velocity was varied from 0.4 to 1 m/s. Schematic of dry sliding test is shown in Fig. 1. The counterface disk was made up of ground stainless steel (AISI 314) with centre line average roughness of 0.6 μm.

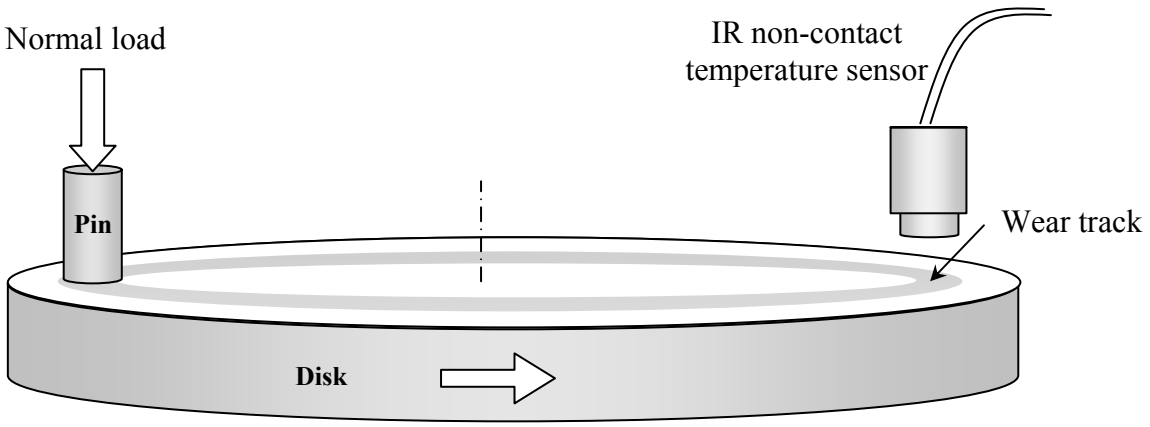

Fig. 1 Schematic of dry sliding test.

Test samples in the shape of cylindrical pins were used in the as-moulded condition. Sliding wear tests were conduced up to sliding distance of 6000 m. Prior to the test the sliding surface was cleaned using acetone and dried. The mass of the pin before and after test were measured using a precision mass balance with an accuracy of 0.0001 g.

The parameters measured on-line during testing are the friction force and the disk temperature. Tests were carried out at room temperature. Wear loss represented as specific wear rate (*K*) is quantified from the mass loss during sliding using Eq. 1.

$$K = \frac{(m_1 - m_2) \times 1000}{\rho . L . S} \tag{1}$$

where *K* is the specific wear rate (mm^3/Nm), m_1 and m_2 are the initial and the final mass of the pins (g), *L* is the normal load (N) and *S* is the sliding distance (m). The coefficient of friction is calculated from the friction force (F) by dividing with the normal load (N). Three tests were conducted for each test condition. After the test, the pins are cleaned to remove any wear debris on the worn surface. The worn surfaces of pins are analysed using scanning electron microscope (SEM) after gold sputtering the surface. The wear track is viewed using optical microscope immediately after test.

DRY FRICTION AND WEAR CHARACTERISTICS

Figure 2 shows the coefficient of friction of PA6 and nanocomposites at a normal load of 50 N and sliding velocity of 0.4 m/s. Owing to the changes in the real area of contact, in most sliding tests, the run-in friction precedes the steady state friction (Kar and Bahadur, 1974). A similar trend was observed in PA6 nanocomposites. The coefficient of friction reaches the steady state after the initial run-in period. The run-in period is characterised by a sudden increase in the coefficient of friction. The effect of clay reinforcement in PA6 is apparent as PA6 nanocomposites exhibit a low steady state coefficient of friction (Fig. 2). As the clay loading increases, the steady state coefficient of friction reduces almost linearly with clay addition. Among the materials tested, PA6 nanocomposite with 5% clay exhibits the lowest coefficient. With 5% clay reinforcement, the average steady state coefficient of friction reduces from 0.45 to 0.25.

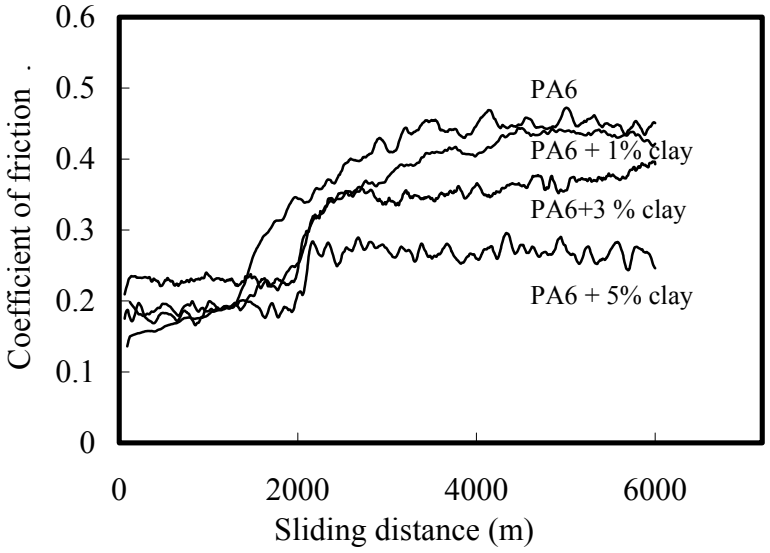

Fig. 2 Effect of sliding distance and clay content on coefficient of friction of PA6 and nanocomposites at a normal load of 50 N and sliding velocity of 0.4 m/s.

During injection moulding of the pin, as the melt cools fast at the surface of the mould, a skin is formed on the pin surface. The skin formed alters the friction behaviour as it is harder and may have different composition (mostly filler rich) than the inner core (Rosato and Rosato, 2003; Bayer, 1994). Hardness measurements at the core and skin indicated an increase in hardness at the surface in all the samples. Due to the presence of hard skin, the coefficient of friction of all materials is low initially and once the skin is removed during sliding, the soft inner core is exposed and the friction coefficient increases. Increase in the normal load disrupts the skin faster and, hence, the run-in region is less. Addition of clay increases the hardness of both skin and core of the pin. As the skin is harder than that of neat polymer, complete shifting of the run-in region has not occurred and it requires higher load to achieve the complete shift.

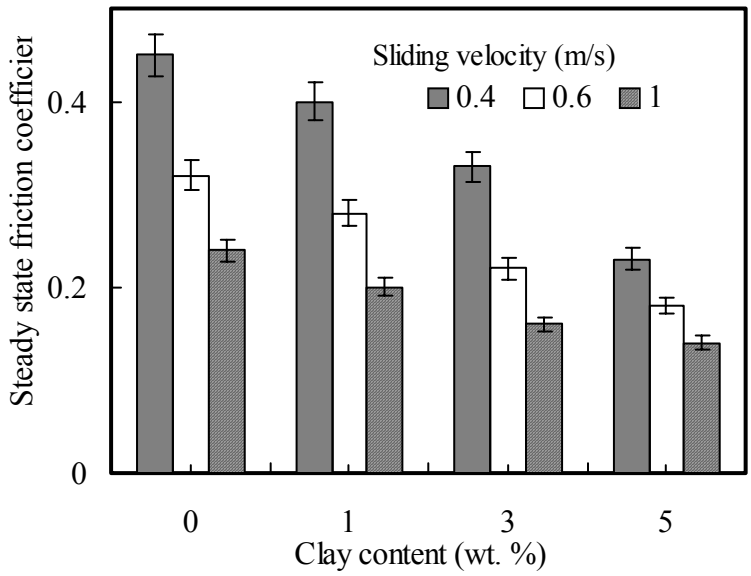

Fig. 3 Effect of sliding velocity on coefficient of friction at a normal load of 50 N.

Figure 3 shows the effect of sliding velocity on the steady state coefficient of friction. As the sliding velocity increases, the coefficient of friction decreases. For neat PA6, the coefficient of friction drops from 0.45 to 0.24 with the increase in sliding velocity. The drop in the friction coefficient with increase in sliding velocity decreases with clay addition. This behaviour is due to the viscoelastic nature of the nanocomposites (Moore, 1975; Hutchings, 1992). As these materials have a time dependent deformation behaviour, increase in the frequency of loading or strain rate tends to make the material stiff (Menard, 1999). The sliding velocity at the asperity level can be linked to the strain rate and increase in the sliding velocity can be considered as increase in the strain rate. Increase in the strain rate at the asperity causes it to be stiffer.

Continuous sliding of the surfaces leads to the generation of heat at the contact point due to friction and leads to the increase in temperature of disk and pin. The net heat build up in polymeric materials reduces the strength and modulus. Moreover, as the polymers are poor conductors of heat, the temperature build up at the surface of the polymer pin. This temperature rise can accelerate the wear process (Sinha, 2002). As

the polymers are viscoelastic, the temperature rise can alter the state of polymer from glassy to viscous when the temperature exceeds the glass transition temperature. Since the counterface is conductive, the heat generated dissipates and increases the bulk temperature of the disk. Hence, the bulk temperature of the disk depends upon the frictional heat dissipation at the interface. Figure 4 shows the temperature rise of the disk due to frictional heating during testing at a normal load of 60 N. Due to the high coefficient of the friction of the pristine PA6, the heat generated in the disk is high and the increase in temperature accounts up to 17 K from the room temperature. With the addition of clay, the rise in temperature decreases and, for PA6 + 5% clay, the rise in the temperature is only 7 K. The temperature initially increases with the sliding distance and reaches a steady state.

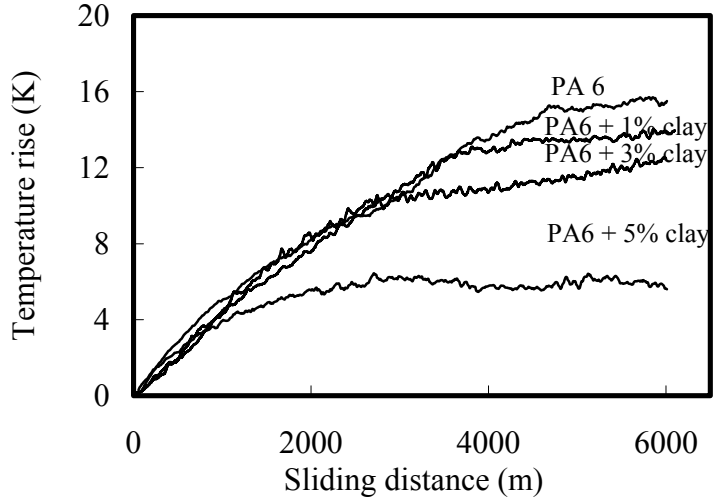

Fig. 4 Rise in temperature of the disk during sliding at normal load of 60 N and sliding velocity of 0.4 m/s

The effect of normal load on the temperature rise of the disk is shown in Fig. 5. The temperature of the disk increases as the frictional heat generation increases with the normal load. Similar to the friction characteristics, the increase in the temperature of disk decreases with the addition of clay.

FRICTION MODEL FOR VISCOELASTIC MATERIALS

In order to model the friction characteristics of nanocomposites from its viscoelastic properties, contact surfaces of two blocks rubbing against each other are considered. Asperities of the composite and steel at the interface will interact with each other giving rise to adhesion and deformation. The interaction between the asperities during sliding is shown schematically in Fig 6.

In the current approach, it is assumed that no wear occurs during sliding and the asperity experiences only elastic deformation and associated hysteresis loss. In addition, as the steel surface is much stiffer than the composite surface, it is considered as rigid and no deformation occurs in the steel asperity. The sequence of loading and unloading experienced by a asperity modelled using Wiechert elements is shown in Fig 7. Here the WM-I whose relaxation modulus is Et represents the normal load while

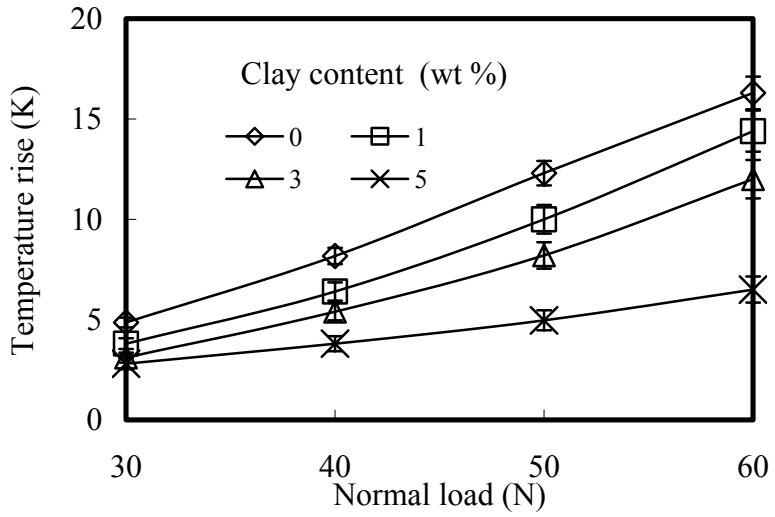

Fig. 5 Effect of normal load on the temperature rise of the disk.

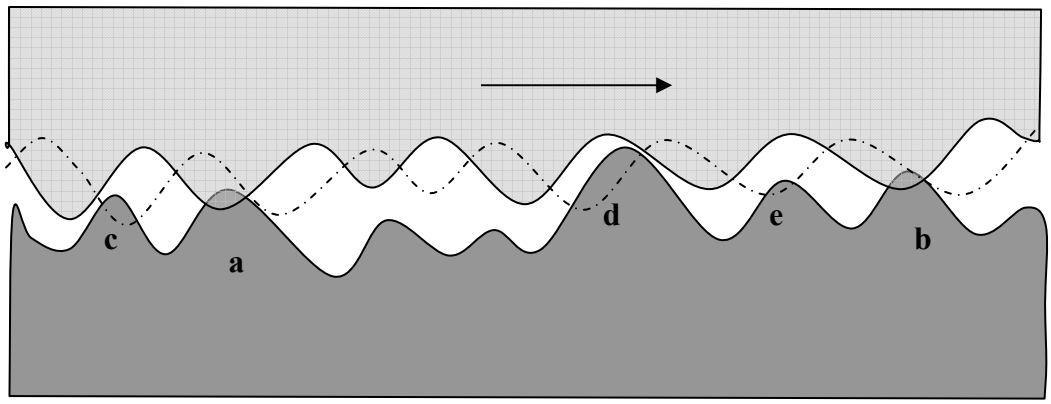

Fig 6. Schematic of asperity interaction of two surfaces in sliding contact

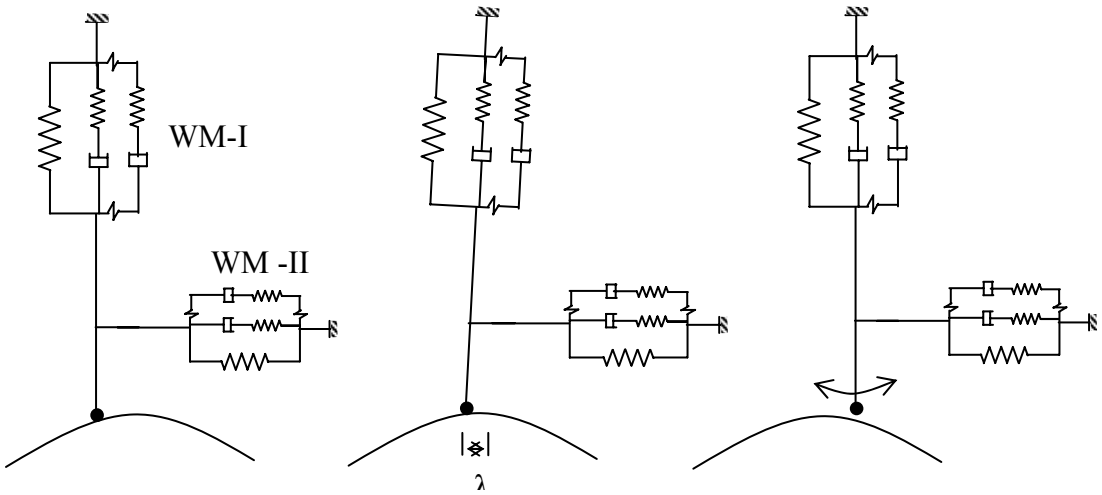

Fig 7 Sequence of loading and unloading of a single asperity using Wiechert elements

WM-II represents shear loading with a relaxation modulus, G_t. When the asperity is loaded normally, the WM -I deforms and while with lateral loading (friction force), the WM-II deforms.

When the asperity contacts the counter face with a normal load, W, it adheres to the counter surface and deforms due to the movement of the asperity. After deforming to a maximum strain, □, the adhesive bond between the asperity and counter face breaks. Then the asperity detaches and returns to its original configuration. During this loading and unloading of the asperity, a part of the strain energy is lost as frictional work. The total work, W_T, done during loading cycle is:

$$W_T = \frac{1}{2} S_{\max} \partial A \lambda \tag{2}$$

where S_{max} is the maximum stress and □□is the contact area. If e is the lost fraction, the energy lost is:

$$W_L = \frac{1}{2} e S_{\max} \partial A \xi \tag{3}$$

The strain increases at a rate, *a*, during the loading cycle, after it reaches the maximum strain, the strain drops to zero suddenly with a strain rate, – *b*, and *b* is much greater than *a*. In order to determine the stress state in a viscoelastic material at a given time, the deformation history of the asperity is considered.

The energy acquired by asperity during loading and unloading can be shown [Srinath, 2007] as

$$E_{load} = \int_0^{\lambda} \sigma_1(\varepsilon) d\varepsilon \quad = \int_0^{\frac{\lambda}{a}} \sigma_1(t) a dt \tag{4}$$

$$E_{unload} = \int_{\varepsilon_{\sigma=0}}^{\lambda} \sigma_2(\varepsilon) . d\varepsilon \quad = \int_{t_{\sigma=0}}^{\frac{\lambda}{a}} \sigma_2(t) . b . dt \tag{5}$$

Here $t_{□=0}$ is the time at which the stress becomes zero during unloading cycle. The energy lost during the process:

$$E_{lost} = E_{loading} - E_{unloading} \tag{6}$$

The lost fraction, *e*, is

$$e = \frac{E_{lost}}{E_{load}} \tag{7}$$

This energy loss is equated to the friction work done (Eqns 3 and 7) and simplifying

$$F = \frac{1}{2} e S_{\max} \partial A \tag{8}$$

where F is the friction force.

From the Hertzian contact theory, for a viscoelastic contact [Hui *et al.,* 2000], the contact area ∂A of viscoelastic sphere on rigid surface is:

$$\partial A \propto \frac{W}{E_r(t)} \tag{9}$$

where W is the normal load and E_r(t) is the relaxation modulus. Hence, Eq 8 becomes

$$F = k\frac{eS_{\max}W}{E_r(t)} \tag{10}$$

where k is geometry factor of the asperity.

Eq 10 gives the friction force on one asperity. In a real surfaces having 'N' asperity contacts under going similar deformation history, the total friction force F_T is given by:

$$F_T = \frac{W}{E_r(t)}\sum_{i=1}^{N} k_i S_{\max_i} e_i \tag{11}$$

Coefficient of friction, $\mu = F_T/W$, and hence,

$$\mu = \frac{1}{E_r(t)}\sum_{i=1}^{N} k_i S_{\max_i} e_i \tag{12}$$

Assuming all the asperities encountering same strain history as that of the single asperity considered, Eq 12 becomes:

$$\mu = \frac{eS_{\max}}{E_r(t)}\sum_{i=1}^{N} k_i \tag{13}$$

The factor $\sum_{i=1}^{N} k_i$ represents the sum of the geometry factors of all the N asperities.

If different materials are tested, having same number of asperities and geometry factor, the coefficient of friction depends on factor, $\frac{eS_{\max}}{E_r(t)}$. Addition of clay to PA6 matrix alters the mechanical properties and hence the coefficient of friction. In order to find out the effect of clay reinforcement (1, 3 and 5%) in PA6 matrix, the ratios of the factor $\frac{eS_{\max}}{E_r(t)}$ of PA6 and nanocomposites are calculated:

$$\mu_{0\%} : \mu_{1\%} : \mu_{3\%} : \mu_{5\%} = \left.\frac{eS_{\max}}{E_r(t)}\right|_{PA6} : \left.\frac{eS_{\max}}{E_r(t)}\right|_{PA+1\%clay} : \left.\frac{eS_{\max}}{E_r(t)}\right|_{PA+3\%clay} : \left.\frac{eS_{\max}}{E_r(t)}\right|_{PA+5\%clay} \tag{14}$$

Assuming the strain under elastic limit for polymers as 1% ($\dot{\varepsilon}$ 0.01) and strain rate as 0.4 s^{-1}, the E_r at time $\frac{\lambda}{a}$ is evaluated using Eq 10. Eq 14 is normalised by dividing the

factor $\frac{eS_{\max}}{E_r(t)}$ of PA6 in order to find the effect of clay reinforcement in PA6 matrix. Hence, Eq 14 becomes:

$$\mu_{0\%}/\mu_{0\%}: \mu_{1\%}/\mu_{0\%}: \mu_{3\%}/\mu_{0\%}: \mu_{5\%}/\mu_{0\%}=1: 0.61: 0.45: 0.38 \quad (15)$$

Eq 15 shows that $\mu_{1\%}= 0.61\mu_{0\%}$, $\mu_{3\%}= 0.45\mu_{0\%}$ and $\mu_{5\%}= 0.38\mu_{0\%}$. This means that irrespective of load applied, ratios of the coefficient of friction of nanocomposites vary by the ratio given. Addition of 1% clay in PA6 matrix reduces the coefficient of friction by 0.61 times while 3% clay reduces by 0.45 times and 5% clay addition reduces by 0.38 times as long as elastic contact condition prevails at the interface.

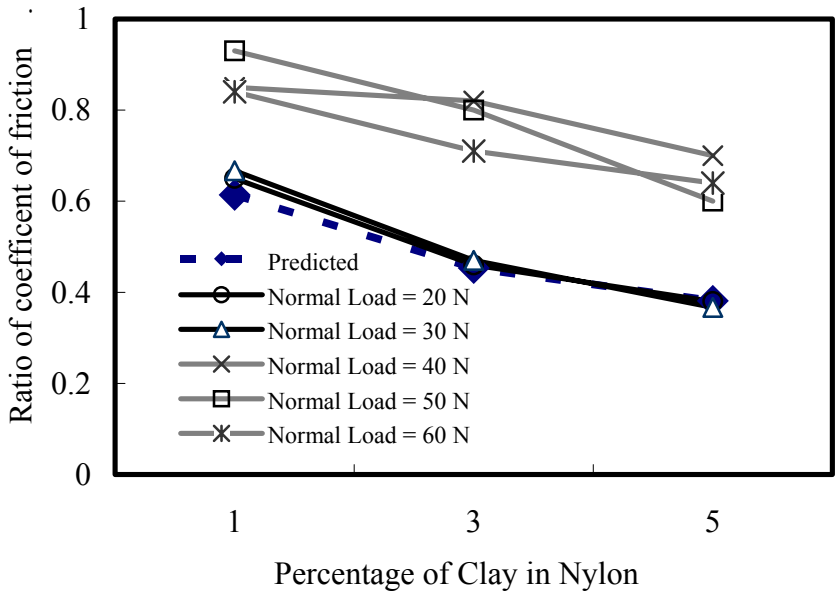

Fig 8 Effect of clay addition on the ratio of coefficient of friction

Figure 8 shows the measured and the predicted ratios of coefficient of friction of nanocomposites to coefficient of friction of PA6. The evaluated ratios of coefficients of friction are in reasonable agreement with the measured values at low loads. However, differences occur at high loads. At high loads, both elastic and plastic deformation occurs in the asperity. As the present model considers only elastic deformation of one asperity, evaluated ratios agrees well at low loads. Also in the model, material removal (wear) and formation of transfer layer are not considered, which also have an effect on the friction process of the nanocomposites.

CONCLUSIONS

Based on the studies carried out to understand the tribo behaviour of polyamide base nanocomposites following conclusions are arrived.

Clay loading effectively reduced the coefficient of friction and wear and the reduction was almost linear with the clay content. The formation of skin on the surface of pin

affects the friction properties of PA6 nanocomposites. Addition of clay increases the hardness of the skin. Formation of uniform tenacious transfer layer and high crystallinity of nanocomposites reduces the wear.

A model to predict the coefficient of friction based on single asperity contact is developed the. The ratio of coefficient of friction of nanocomposites to the coefficient of friction of pristine PA6 was found using the model and it was in reasonable agreement with the measured values at low loads. The strain rate has a major effect on the friction coefficient. Increase in the strain rate causes the materials to be stiffer and reduces the coefficient of friction.

REFERENCES

Bayer, R.G. *Mechanical Wear Prediction and Prevention*. Marcel Dekker Inc, New York, 1994.

Hui, C.Y., Y.Y. Lin and **J.M. Bany** (2000) The mechanism of tack: Viscoelastic contacts on a rough service, *Journal of polymer science: Part B: Polymer Physics*, **38**, 1485-1495.

Jordan, J., K. I., Jacob, R. Tannenbaum, M.A. Sharaf and Iwona Jasiuk (2005) Experimental trends in polymer nanocomposites-a review. *Materials Science and Engineering A*, **393**, 1-11.

Kar, M.K. and S. Bahadur (1974) The wear equation for unfilled and filled polyoxymethylene, *Wear*, **30**, 337-348.

LeBaron, C.P., Zhen Wang and T.J. Pinnavaia (1999) Polymer-layered silicate nanocomposites: an overview, *Applied Clay Science*. **15**, 11-29.

Li, F., Ke-ao Hu, Jian-lin Li and Bin-**yuan Zhao** (2002) The friction and wear characteristics of nanometer ZnO filled polytetrafluroethylene, *Wear*, **249**, 877-882.

Menard, K.P., *Dynamic mechanical analysis – A practical introduction*, CRC Press, Boca Raton, 1999 **Sinha, S.K.**, *Wear failure of plastics*, pp 1020-1027 *In* **J. Hawk**, **R. Wilson**, **W.T. Becker** and **R.J. Shipley** (eds.) *ASM handbook Vol 11 Failure analysis and prevention*, ASM international, *Materials Park*, 2002.

Rosato, D.V. and **D.V. Rosato**, *Plastics engineering product design*, Elsevier, Oxford, 2003.

Schwartz, C.J. and **S. Bahadur** (2000) Studies on the tribological behaviour and transfer film-counterface bond strength for polyphenylene sulphide filled with nanoscale alumina particles, *Wear*, **237**, 261-273.

Srinath, S, *Tribo behaviour of polyamide 6 layered silicate nanocomposites,* Doctoral Thesis, Indian Institute of Technology Madras, India, 2007.

Wang, Q., Jinfen Xu, Weichang Shen and **Weimin Liu** (1996a) An investigation of friction and wear properties of nanometer Si_3N_4 filled PEEK, *Wear*, **196**, 82-86.

Xue, Q. and **Qi-Hua Wang** (1997) Wear mechanisms of polyetheretherketone composites filled with various kinds of SiC, *Wear*, **213**, 54-58.